J Solid State Electrochem (2011) 15:593–600
DOI 10.1007/s10008-010-1127-4

ORIGINAL PAPER

Spectroscopic and impedance studies of reverse biased degraded dye solar cells

Lukas Johannes le Roux · Dirk Knoesen · Sibbele Hietkamp

Received: 18 December 2009 / Revised: 9 June 2010 / Accepted: 13 June 2010 / Published online: 30 June 2010

Abstract The work that is presented here is focused on the results that were obtained during studies of the performance of dye solar cells under certain reverse bias conditions. This reverse voltage could permanently modify or damage a cell if it is not properly protected. Various techniques were employed to determine the physical changes in the cell. It was found that a cell that was subjected to a reverse bias of 2 V for 500 min showed a 58% recovery. The UV-vis spectra showed a blue shift (higher energy), the Raman showed no peak at 1,713 cm^{-1} and the FT-IR showed the disappearance of the S-C-N absorption band at 2,100 cm^{-1}. The combined conclusion is that the NCS ligand has been depleted and replaced with I_3^- ions. Nyquist and Bode plots showed an increase in the charge transfer resistance at the counter electrode. This indicates a partial oxidation of the Pt catalyst on the counter electrode. The changes in the cell after being subjected to a reverse bias potential of 2 V for 500 min are changes on the NCS bonds on the Ru containing dye as well as the Pt on the counter electrode.

Keywords Electrochemical impedance spectroscopy · Nyquist plots · Bode plots · IV curves · Raman · FT-IR · UV-vis · Reverse bias

Introduction

A dye solar cell is an electrochemical cell that generates electricity when light excites the electrons in a ruthenium containing dye (from hereon called the Ru dye) that is chemically adsorbed on a thin layer of nano-TiO_2. It consists of a working electrode (TiO_2 and dye), an electrolyte (0.1 M I_2, 0.1 M LiI, 0.6 M tetrabutylammonium iodide, 0.5 M 4-*tert*-butylpyridine in acetonitrile) and a counter electrode (platinum catalyst).

L. J. le Roux (✉) · D. Knoesen · S. Hietkamp
CSIR Materials Science and Manufacturing,
Energy and Processes,
PO Box 395, Pretoria 0001, Africa
e-mail: lleroux@csir.co.za

Reverse bias

Reverse bias conditions occur when the voltage across a cell opposes the open circuit potential. A multi-cell module might have one or more of its cells shaded out while operating in the open. When one cell in the series connection is shaded, the current will pass this cell in reverse bias. An example of such a case can be seen in Fig. 1. In such a case the shaded cell will be subjected to a voltage in the reverse direction coming from the other lit cells in the module. The reverse voltage could adversely modify or damage the cell if it is not properly protected.

When a negative voltage is applied, the potential across the semiconductor increases as well as the depletion layer width. When a positive voltage is applied, the potential across the semiconductor and the depletion layer width will decrease. The total potential across the semiconductor equals the built-in potential minus the applied voltage (Fig. 2).

According to Kern et al. [1], reverse biasing a dye solar cells (DSC) is not critical for stability thus integrated modules are possible without protection diodes on each cell.

A test example of a dye solar cell was accidentally subjected to a reverse bias potential of 6 volts for a few seconds. The efficiency was immediately measured and found that the cell was dead. The following day, the cell was tested again and unexpectedly it was found that a certain degree of recovery or regeneration had taken place.

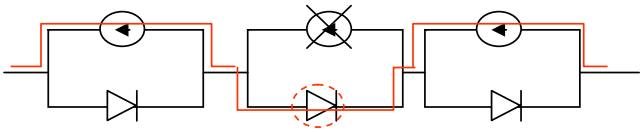

Fig. 1 Example of the circuit where one cell is shaded

In real life situations, one or more cells in a module can be partially shaded, which results in electrical mismatching in the cell. The cell is then subjected to reverse bias. The electrons then flow into the cell instead of out. This could irreversibly damage the cells if the voltage is large enough. To prevent damage to cells due to reverse bias, diodes are incorporated in the circuit to prevent any possibility of reverse bias. This research looks at the effects that reverse bias has on DSCs and the physical and chemical changes that occurred as a result of reverse bias.

Wheatley et al. [2] reported a similar incident but it was not pursued in so much detail. They used Raman, UV-vis and cyclic voltammetry to determine changes that possibly took place in the cells. They concluded (cyclic voltammetry) that some irreversible oxidation process occurred inside the cell.

Dye solar cells were subjected to different reverse bias potentials (1, 2, 2.5 and 4.5 V). This paper reports on the results that were obtained for a cell that was subjected to a reverse bias potential of 2 V for 500 min.

Spectroscopic techniques (UV-vis, Raman, Fourier transform infrared (FT-IR) and scanning electron microscope (SEM)) were complimented by electroanalytical methods (impedance and current–voltage (IV) curves), and used to determine the physical and chemical changes that caused the decrease in cell efficiency.

Experimental

Various cells (at least five of each) were assembled to assure repeatable results of the tests.

The cell dimensions were 8 mm×60 mm (4.8 cm^2). The dye (Fig. 3) that was used in all cases was the N719 {di-tetrabutylammonium cis-bis(isothiocyanato)bis(2,2′-bipyridyl-4,4′-dicarboxylate) ruthenium(II)} as supplied by Dyesol. The ITO conductive glass was purchased from Solaronix (8 Ω/square).

A Perkin Elmer, Lambda 750S UV/vis spectrometer was used to obtain the UV/vis reflectance and absorbance spectrographs as part of the characterisation of the cells. The shift and intensity of the absorption band at 540 nm due to reverse bias was investigated, over a scan range of 400 to 700 nm at a scan rate of 266.7 nm/min and a resolution of 1 nm.

The FT-IR spectral data were collected on a Perkin Elmer Spectrum 100 FT-IR spectrometer interfaced with a Spectrum Spotlight 400 FT-IR imaging system. The changes in the NCS vibration band at 2100 cm^{-1} and C=O vibration bands at 1,715 and 1,354 cm^{-1} were monitored over 64 scans per sample at a resolution of 4.00 cm^{-1} in attenuated total reflectance mode.

The Raman signal is characteristic of a particular functional group. This function would enable us to study the degradation of the dye in the cell during reverse bias [3]. Raman spectra were obtained with Jobin Yvon Lab Ram HR800 spectroscopy at room temperature, and samples were excited using the 514.5 nm line. The spot size was 150 μm, and the laser power was 2 mW. The acquisition time per sample was 60 s. The microscope magnification was 10×, and the system was interfaced with an Olympus BX 41 camera. The three characteristic vibration bands at 1,472, 1,540 and 1,610 cm^{-1} were used to indicate changes in the Ru–bipyridyl bonds.

Particle and surface morphologies were studied by scanning electron microscopy using a JEOL JSM 7500F Field Emission Scanning Electron Microscope. The nano-TiO_2 that was synthesised in our laboratories was compared with the P25 that was obtained from Degussa South Africa. The surfaces of the cells were compared before and after the reverse bias experiments.

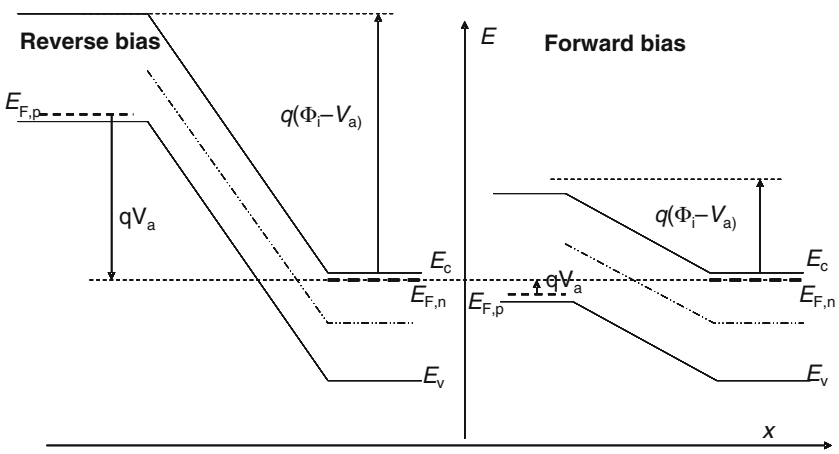

Fig. 2 Schematic energy diagram of the change in energy levels when a cell is subjected to reverse and forward bias E_c= energy at the conduction band E_F=Fermi energy level E_v=energy at the valence band N_a= acceptor density in the *p* type region per cm^3 N_d=amount of donors in the *n*-type region per cm^3 n_i^2=amount of positive (or negative) charge carriers per cm^3 V_f=k_bT/q (volts) k_b=Bolzmann's constant 1.38×10^{-23} JK^{-1} k_bT= kinetic energy in eV *q*=charge of an electron 1.602×10^{-19} C

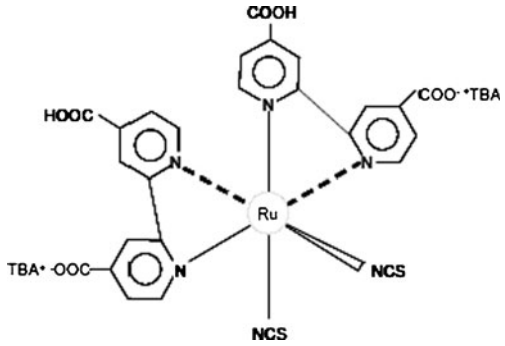

Fig. 3 Structure of the N719 dye

The IV characteristics of the solar cells were monitored and recorded with the use of a mobile testing station for photovoltaics (MTSP purchased from Dyesol, Australia) and the solar simulator was obtained from Sciencetech (USA). The cells were scanned from −0.1 V to 0.8 V which was plotted against the current. All measurements were done under irradiation of one sun (1 kWm^{-2}).

The electrochemical measurements were carried out in the dark using a PGSTAT 12/30/230 potentiostat. A two electrode configuration was used where the sensitised TiO_2 was connected as the working electrode while the counter electrode (Pt), doubled as the reference electrode. The scan rate was 50 mV/s. The bias potentials ranged from −0.7 to +0.7 V.

Results and discussion

Reverse bias and recovery

The results of four identical cells that were subjected to different reverse bias voltages and the efficiencies were plotted against time are shown in Fig. 4. Reverse bias voltages of 1 V (blue); 2 V (Magenta); 2.5 V (black); and 4.5 V (brown) were used in the experiments.

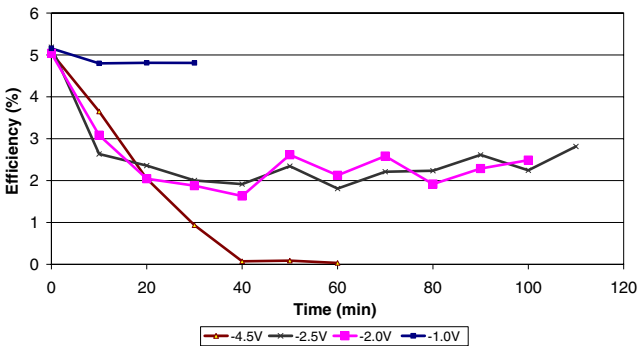

Fig. 4 Efficiencies plotted during subjection to different reverse bias voltages. Measurements were taken at 10-min intervals. Note the similar results for 2 and 2.5 V

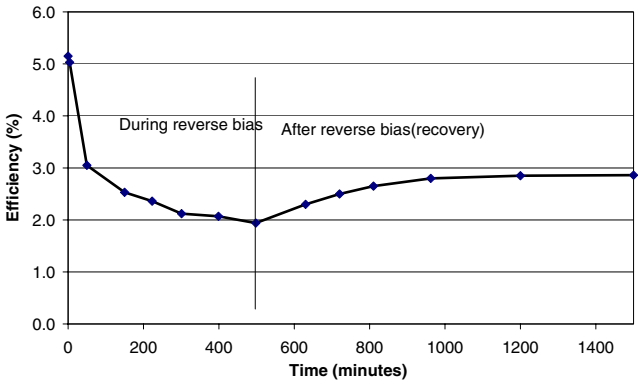

Fig. 5 A plot of efficiency vs. time for a cell that was subjected to a reverse bias of 2 V for 500 min after which the cell's recovery was monitored

Under a reverse bias of 1 V, there is little reduction in the efficiency of the cell. The drop in efficiency from 5.1% to 4.8% is 0.3% (5.9% overall).

Figure 4 shows that there was no meaningful difference when the cells were subjected to reverse bias voltages of 2 and 2.5 V. The results for the 2.5 V reverse bias experiments will therefore not be discussed further in this document.

When the cell was subjected to a reverse bias potential of 4.5 V, the efficiency dropped to 0% in 50 min.

A cell was subjected to a reverse bias potential of 2 V and the efficiency was measured at different time intervals to determine the rate of degradation. The regeneration was measured against time after the reverse bias voltage was removed. The efficiencies were plotted against time (see Fig. 5).

The efficiency of the cell decreased from 5.1% to 2% after 500 min. When the reverse bias potential was removed, the cell recovered partially to give a final efficiency of 2.9%.

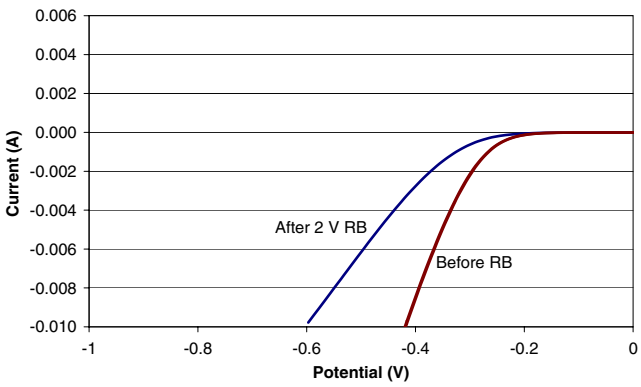

Fig. 6 The IV curves for the cells (negative voltages only). The red line represents the cell that was not subjected to any reverse bias. The blue line is the cell that was subjected to 2 V reverse bias

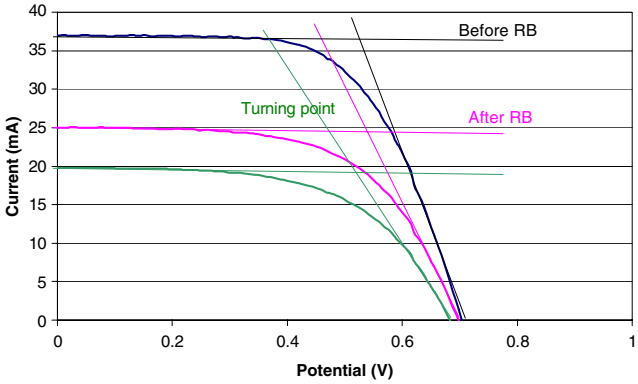

Fig. 7 IV curves for the cell during and after being subjected to a reverse bias of 2 V. The blue trace is the efficiency before reverse bias while the recovered is indicated by the magenta trace. The green trace represents the turning point before recovery. The slopes of the I_{sc} and V_{oc} are also indicated on the graph

The data from the graph (Fig. 6) was used to determine the different values for the exchange current density. This was compared with the curve of the cell before reverse bias. The Butler–Vollmer model is only valid in reverse bias (V<0) [4].

$$J(V) = J \circ \underbrace{\left(\exp\left(\beta \frac{qV}{kT}\right)\right)}_{\sim 0 \text{ for } V<0} \quad (1)$$

Applying the experimental data to the simplified Butler–Volmer equation, the following values were calculated for J_0 (exchange current density). The symmetry factor (β) was taken as 0.5. J_0 is indicative of the rate of oxidation or reduction at an equilibrium electrode. J_0 for the cells were determined as:

Before reverse bias: 7.2×10^{-11} A/cm^2; after 2 V reverse bias: 8.8×10^{-13} A/cm^2

The reaction rate after the cell was subjected to a reverse bias potential of 2 V was about three times less than the cell before reverse bias.

Efficiency measurements

The IV curves shown in Fig. 7 were obtained during the time that the cell was subjected to reverse bias. The blue traces are during reverse bias while the recovery is indicated by the magenta traces. Although there was a significant change in the I_{sc}, the V_{oc} showed only a small variation.

The inverse of the slopes of the curve that indicates R_{sh} and R_s are shown in Table 1.

These values show the same trends that were found when the modelling was done for the equivalent circuits (see Table 2).

Table 1 Shunt and series resistances as calculated from the IV curves

	R_{sh} (Ω)	R_s (Ω)
Before reverse bias	3,324	4.3
Minimum efficiency (turning point)	2,517	7.6
After recovery	3,247	5.8

Table 2 Numerical values (based on the model of the Nyquist plot) of the different components of the cells before and after reverse bias

	Before reverse bias	After reverse bias of 2V
R_1	4.73 Ω	4.73 Ω
C_1	1.00 pF	1.00 pF
R_2	12.8 mΩ	15.4 mΩ
R_3	4.73 Ω	4.73 Ω
C_2	22.8 μF	1.00 pF
R_4	46.8 Ω	146 Ω
Q_1	$4.40\times10^{\times-4}$	7.98×10^{-4}
n_1	0.833	0.827
R_5	4.73 Ω	4.73 Ω
C_3	10.6 μF	1.00 pF
Q_2	4.46×10^{-4}	7.97×10^{-4}
n_2	0.834	0.829
R_6	61.3 Ω	208 Ω

R_1, R_3 and R_5 are the series resistance components of the cell and showed no change before or after reverse bias of 2 V. The major differences appear to be with the charge transfer resistance (R_2, R_4 and R_6) that indicates that physical changes took place inside the cell as well as at the counter electrode.

Impedance measurements

Note there is no significant change in the series resistance (R_s), indicated on the right hand side of the graph in Fig. 8. Both start at 1.4 Ω. After the cell was subjected to 2 V reverse bias, the charge transfer resistance (R_{ct}) increased to 340 Ω.

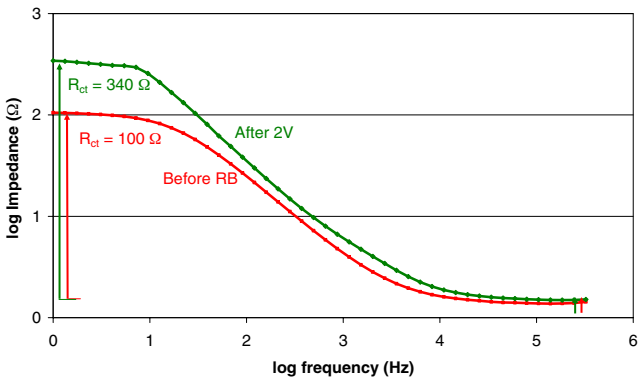

Fig. 8 Bode plots of the cell before reverse bias (*red*) and after 2 V reverse bias (*green*)

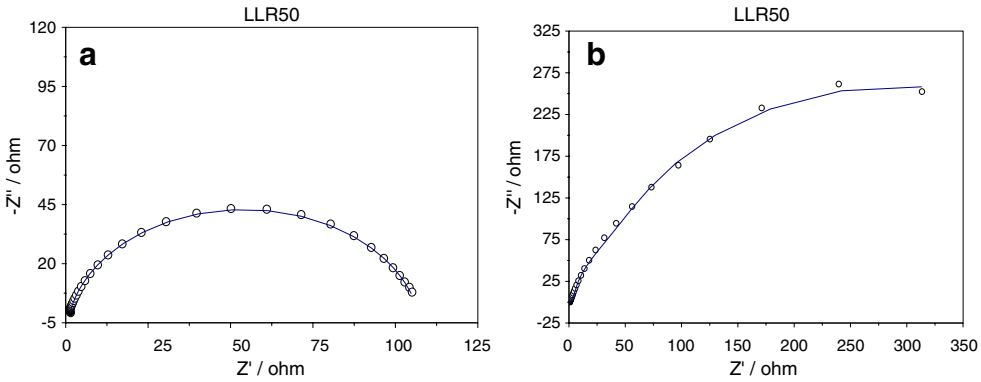

Fig. 9 Nyquist plots of the cells cell before (**a**) and after (**b**) reverse bias. The *blue lines* show the theoretical fit of the equivalent circuit in each case

The increase in impedance shown in Fig. 8 also correlates with the trends of increase in impedance that is depicted in the Bode plots (Fig. 8). Figure 9 shows the Nyquist plots as well as the equivalent circuits of the cells before and after reverse bias.

The equivalent circuits for both cases are essentially the same as shown in Fig. 10. The circuits give a good fit as shown in the Nyquist plots (Fig. 9). The calculated values of the components (before and after reverse bias) that are derived from these models are compared in Table 2.

The part of the circuit that is shown as R_2, represents the charge transfer resistance for electron recombination at the TiO_2/ITO interface in the cell while C_1 represents the capacitance at the triple contact ITO/TiO_2/electrolyte.

$C_2/R_4/Q_1$ represents the charge transfer resistance (R_4) due to the recombination of electrons at the TiO_2/electrolyte interface, the chemical capacitance (C_2) and constant phase element (Q_1) due to a change in electron density. (The first indication that a constant phase element exists is that the centre of the semi circle in the Nyquist plot has shifted to below the *x*-axis.) This is evident in both plots in Figs. 9 and 11.

R_3 and R_5 represent the electron transport resistance in the TiO_2 layer. $C_3/Q_2/R_6$ represents the capacitance and charge transfer resistance as well as the constant phase element at the electrolyte/platinum interface in the cell.

The charge transfer resistance at the electrolyte/platinum interface increased from 61 Ω to 208 Ω. Work that was done by Milkevitch et al. [5] indicated that the platinum catalyst can be irreversibly oxidised at voltages of 1.72 V and 1.61 V. The value of the constant phase elements Q_1 and Q_2 doubled while the value of n only increased slightly from 0.827 to 0.833 which relates to 0.5° change in the phase. The capacitance inside the cell (C_2 and C_3) has decreased significantly while the capacitance at the working electrode stayed constant.

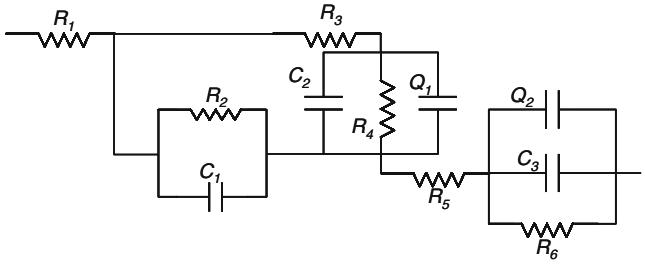

Fig. 10 Equivalent circuit of a cell before and after reverse bias

UV-vis measurements

When a reverse bias potential of 2 V was applied to the cell the absorption band at 540 nm shifted to 525 nm with a reduction in absorptivity (Fig. 12). This absorption band is due to the metal-to-ligand charge transfer from the Ru metal centre to π* orbitals on the pyridyl ligand. The molecule is stabilised by the delocalising effect of the electron donating N-C-S groups. The band shifted to higher energy (blue shift) which resulted in lower cell efficiency.

The absorbance decreased from 0.68 to 0.47 (30%). The decrease in cell efficiency was 42% (from 5.1% to 2.9%) which suggests that this is not the only parameter that changed during the reverse bias.

It was previously determined by Murakoshi et al. [6] that the absorption shifts to lower energies when the complexes are attached to the semiconductor surface. The band shifts were ascribed to the interaction between the dye

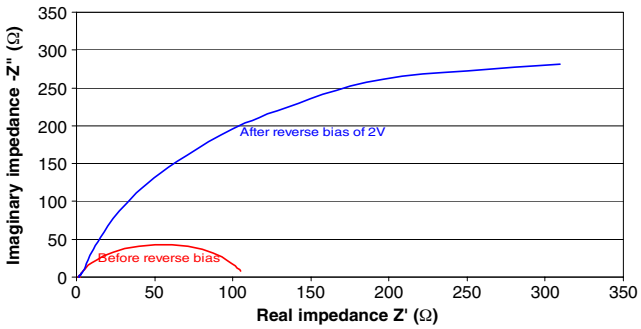

Fig. 11 Nyquist plots of the cell before reverse bias (*red*), after 2 V reverse bias (*blue*)

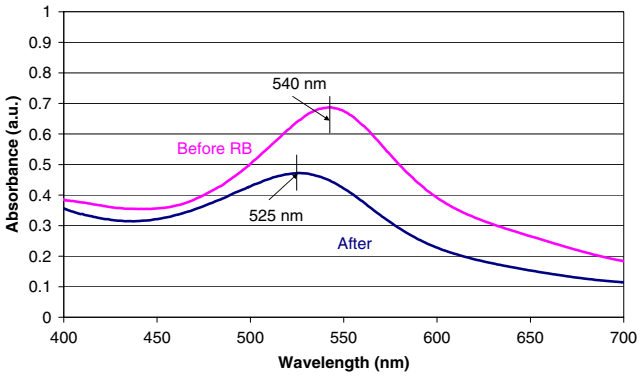

Fig. 12 UV-vis results of a cell before and after reverse bias. Note the peak shift from 540 to 525 nm

molecule and the TiO_2 surface through the carboxylic groups. This leads to the possible conclusion that some of the dye was desorbed from the TiO_2 during the reverse bias experiments.

The blue shift could therefore be a combination of the breaking of bonds between the dye and the TiO_2 and the depletion of the N-C-S groups. It was confirmed by FT-IR and Raman that there is no evidence of bond breaking between the TiO_2 and the dye therefore the shift has to be due to the depletion of the N-C-S groups.

Raman measurements

The absence of the characteristic C=O stretch band at 1,713 cm^{-1} is an indication that there are no free C=O

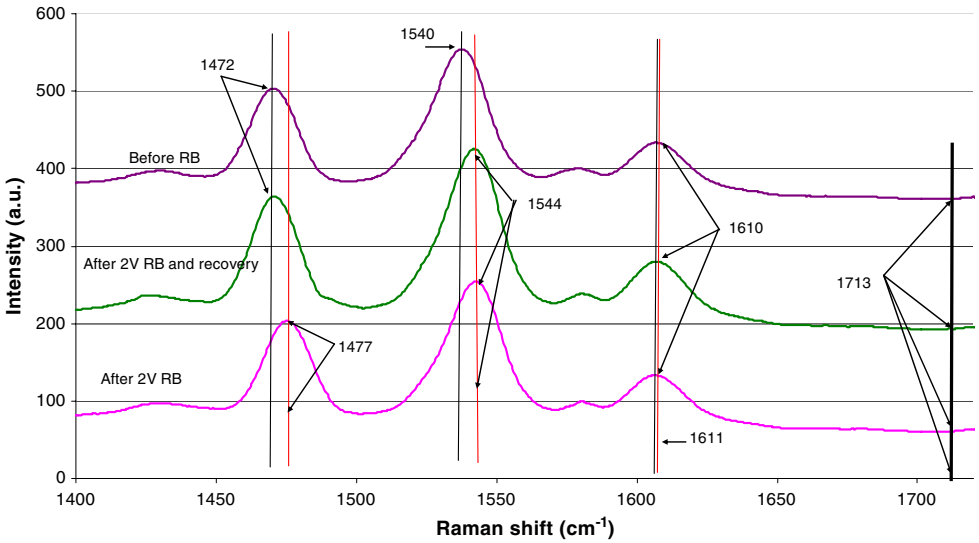

Fig. 13 Raman spectra of a cell that was subjected to a reverse bias voltage of 2 V. Note the peak shifts in the original spectrum before reverse bias, after 2 V reverse bias (before and after recovery). Note the absence of peaks at 1,713 cm^{-1}

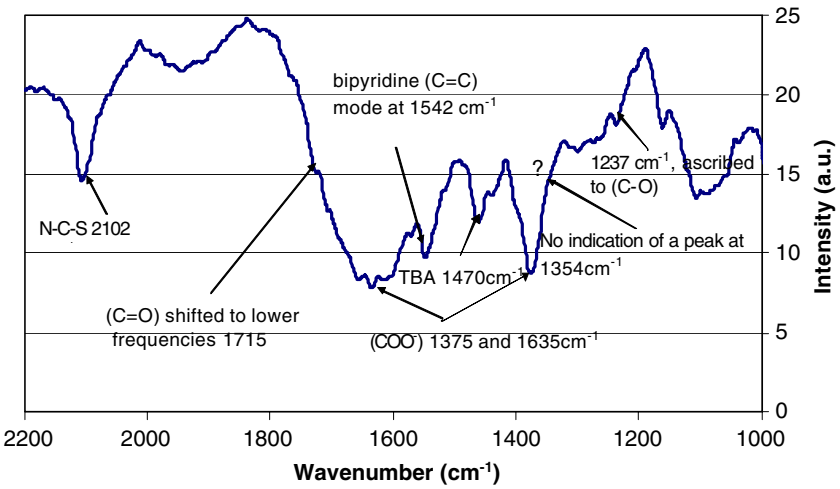

Fig. 14 FT-IR spectrum of the dye after being subjected to a reverse bias voltage of 2 V

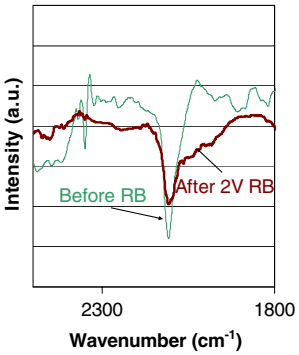

Fig. 15 The FT-IR spectrum of the cells before and after a reverse bias (RB) voltage of 2 V. Note the decrease of the intensity of the CN peak at 2,100 cm^{-1}

groups in the cell. This proves that the dye is not desorbed from the titanium dioxide surface. FT-IR spectroscopy measurements also indicated that no desorption of the dye from the TiO_2 film occurred. During the application of reverse bias potentials, the peaks at 1540 and 1,472 cm^{-1} shifted by 5 and 4 cm^{-1}, respectively, to higher energy while the energy of the band at 1,610 cm^{-1} was essentially unchanged (Fig. 13). After reverse bias and recovery (2 V), the 1,472 cm^{-1} band returned to the original value but the peak initially at 1,540 cm^{-1} remained displaced by 4 cm^{-1} to higher energy. The irreversible change to the band at 1,540 cm^{-1} suggests that the adsorbed dye has undergone a change directly associated with the bipyridyl ligand.

FT-IR measurements

The FT-IR measurements showed n No evidence could be found of any desorption of the dye carbonyl group from the TiO_2. If there were any isolated (not bound to TiO_2) carbonyl groups, vibrational bands at wavenumbers 1,354 and 1,715 cm^{-1} should become evident. This however is not the case. The strong bands at 1,375 and 1,635 cm^{-1} indicate bonded carbonyl groups. Therefore with the FT-IR spectral data we can state that there is no disengagement of the dye from the TiO_2 (Fig. 14). This is also confirmed by results that were obtained by Kuang et al. [7].

The spectra in Fig. 15 show the effect of the 2 V reverse bias on the N-C-S group in the dye. The N-C-S stretching band is slowly depleted. It seems as if the thiocyanate ion ligand is sensitive to the oxidising effect of the reverse bias on the N-C-S groups. It was suggested by Greijer et al., [8] that a compound analogue to the I_3^- forms:

$$I_2 + SCN^- \rightarrow I_2SCN^-$$

This strongly correlates with the decrease in intensity and blue shift in the UV-vis absorption bands and is attributed to the destabilising effect of the depleting N-C-S group.

Scanning electron microscope measurements

SEM photos (magnification for both were 30.00 K X) were obtained before and after the reverse bias potential of 2 V as shown in Fig. 16. No obvious changes or differences could be detected. This confirms that the morphology did not change due to the reverse bias. The surface porosity of the two films does not show any visible or obvious change.

Conclusions

We have shown that a reverse bias potential of 2 V resulted in a 42% loss in cell efficiency.

Raman spectroscopy showed the partial recovery of the cell at 2 V reverse bias. The appearance of a vibration band at 1,713 cm^{-1} would be evidence of the breaking of the chemisorbed bonds between the dye and the TiO_2 film

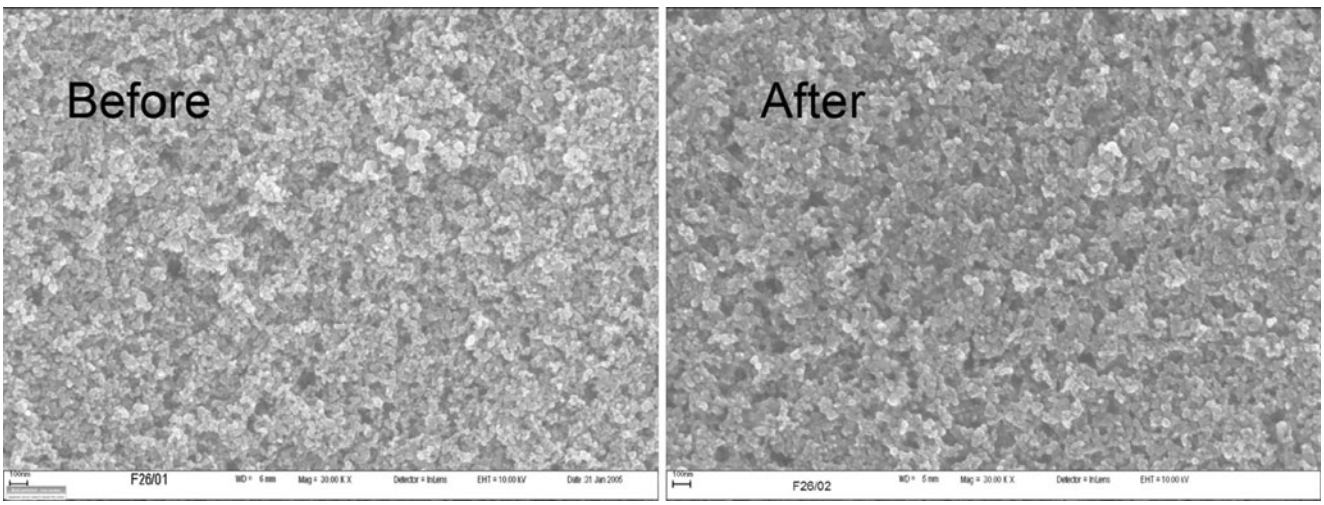

Fig. 16 SEM micrograph of the TiO_2/dye of a cell before and after reverse bias

(dislocation of the dye and the TiO_2). This was not the case and it was also backed up by FT-IR measurements showed no peaks at 1,715 and 1,354 cm^{-1} which is characteristic of free carbonyl bonds.

FT-IR however did show the depletion of the N-C-S vibration band at 2,100 cm^{-1}.

This work has shown that Raman and FT-IR spectroscopy are complementary techniques that provided structural information of the dye and dye/semiconductor system.

Potentiometric measurements show a significant increase in the charge transfer resistance at the counter electrode which indicates a decrease in the catalytic activity of the Pt. This backs the theory of Milkevitch et al. [5] that there is partial oxidation of the Pt that acts as a catalyst for the regeneration of the Iodide. It was shown by FT-IR that the change was in the dye and not the TiO_2/dye bond.

The values of R_s and R_{sh} that were obtained from the IV curves of the cell under reverse bias showed the same trends that were obtained from the Nyquist plots, Bode plots and equivalent circuits.

It can therefore be stated with confidence that the changes in the cell after being subjected to a reverse bias potential of 2 V for 500 min are attributed to changes on the N-C-S groups on the Ru dye as well as the Pt on the counter electrode.

The morphology of the TiO_2 film on the glass substrate does not change when a cell is subjected to a reverse bias potential of 2 V.

Acknowledgements Dr Mkhulu Mathe (Council for Scientific and Industrial Research)

Dr Kenneth Ozoemena (Council for Scientific and Industrial Research/University of Pretoria)

Ms Nonhlanhla Mphahlele (Council for Scientific and Industrial Research)

Ms Nomthandazo Mutangwa (Council for Scientific and Industrial Research)

Dr Paul Sommeling (Energy Research Centre of the Netherlands)

References

1. Kern R, Sastrawan R, Ferber J, Stangl R, Luther J (2002) Modelling and interpretation of electrical impedance spectra of dye solar cells operated under open-circuit conditions. Electrochim Acta 47:4213–4225
2. Wheatley MG, McDonagh AM, Brungsa MP, Chaplina RP, Sizgekc E (2003) A study of reverse bias in a dye sensitised photoelectrochemical device. Sol Energy Mat Sol Cells 76:175–181
3. Gao K, Wang D (2007) Raman study of photo-induced degradation of the Ru(II) complex adsorbed on nanocrystalline TiO_2 films. Phys Status Solidi RRL 1(2):R83–R58
4. Hinsch A, Belledin U, Brandt H, Einsele F, Hemming S, Koch D, Rau U, Sastrawan R, Schauer T (2006) Glass frit sealed dye solar modules with adaptable screen printed design. Paper presented at the 4th World Conference on Photovoltaic Energy Conversion: Hawaii
5. Milkevitch M, Brauns E, Brewer KJ (1996) Spectroscopic and Electrochemical Properties of a Series of Mixed-metal d6, d8 Bimetallic Complexes of the Form [(Bpy)2 m(BL)PtCl2]2+ (Bpy= 2, 2′-Bipyridine; BL=dpq (2, 3-Bis(2- Pyridyl)Quinoxaline) Or dpb (2, 3-Bis(2-Pyridyl)-Benzoquinoxaline); M=Osii or Ruii). Inorg Chem 35(6):1737–1739
6. Murakoshi K, Kano G, Wada Y, Yanagida S, Miyazaki H, Matsumoto M, Murasawa S (1995) Importance of binding states between photosensitizing molecules and the TiO_2 surface for efficiency in a dye-sensitized solar cell. J Electroanal Chem 396:27–34
7. Kuang D, Ito S, Wenger B, Klein C, Moser J, Humphry-Baker R, Zakeeruddin SM, Grätzel M (2006) High molar extinction coefficient heteroleptic ruthenium complexes for thin film dye-sensitized solar cells. J Am Chem Soc 128(12):4146–4154
8. Greijer H, Lindgren J, Hagfeldt A (2001) Resonance raman scattering of a dye-sensitized solar cell: mechanism of thiocyanato ligand exchange. J Phys Chem B 105:6314–6320